A Survey on Thermal Updraft Models

Sreekanth Ganapathi Raju Eric Poquillon Emmanuel Rachelson

Abstract

This report presents a survey on the existing Thermal updraft models. These models are studied to perform autonomous soaring simulations that can help in improving aircraft endurance. This work comprises of several existing approaches used in soaring studies to model updrafts as close as possible to reality. The models surveyed here were developed based on data measurements from regions of updrafts. Thermal updrafts in the form of plume rise called as Chimney Thermals, these Chimney thermals in the presence of light horizontal wind characterized by leaning and drifting and finally completely detached Bubble Thermals are the different kind of updrafts presented here. To close, a software tool is developed based on these models. This tool can be used to create updrafts over a given region based on a selected model. The tool simulates a wind field where updrafts will randomly form and vanish. Hence, it can be used in simulation studies to give the effect of updrafts on the aircraft.

1 Introduction and Motivation

During the past few decades with major advancements in precision sensing, fast actuation and autonomous computing, the controllability and automaticity of modern aircrafts have improved to a large extent. This has also increased the number of both civil and military applications of unmanned aerial vehicles (UAVs). However, as the complexity of their tasks is extending, there is a great demand for seeking more possibilities to extend the range and flight duration of UAVs. A key difference between UAVs and manned aircraft is that their endurance is not limited by operator endurance. A promising idea will be use of atmospheric energy in the form of gusts and updrafts to extend aircraft endurance. Its use could significantly augment the mission duration. With the growing demand for innovation in areas of green technology, energy extraction from atmospheric sources will simultaneously conserve fuel or electrical energy.

Autonomous soaring gliders have shown to be greatly efficient in conserving energy from the atmosphere in the form of Thermal updrafts. Thanks to their very efficient aerodynamics with less drag they can significantly improve range. Any autonomous soaring study can be characterized into the atmospheric model consisting of the winds and thermal updrafts, the flight dynamics of the aircraft and the control algorithm governing the automaticity of the flight. The first step is to model the atmosphere and the thermal as close to reality as possible. For this reason, there is a great interest and also a great importance to understand up winds and thermals in the atmosphere. It is important to look into the available work done in the field of thermal updrafts.

Thermal updrafts are raising mass of air from the ground, caused due to temperature variation between the air close to the ground and the air in the atmosphere. These updrafts are thermal convection currents fuelled by radiating heat from the ground. Since thermal updrafts are very complex phenomenon there exist many approaches to calculate the updraft velocity and size of the updrafts. This bibliography survey report comprises of various previous work done in the study of thermal updrafts. The motivation behind this is to understand the existing research in this field and analyze their advantages and disadvantages. The models explained here are purely empirical and are not based on CFD or any other numerical computations. These models are very simple and effective in terms of computation time.

A software tool has also been developed along with this survey, which can be used along with any soaring simulation studies. This tool is parametric in nature with input variables as position and sim-

ulation time. The output variable will be a wind vector at the given point and time. The tool can be directly used as a blackbox to give the effect of updrafts on the aircraft. The data for all graphs and plots shown in this report are generated using this software tool.

This survey report and the software tool are developed as a first step in performing autonomous soaring study.

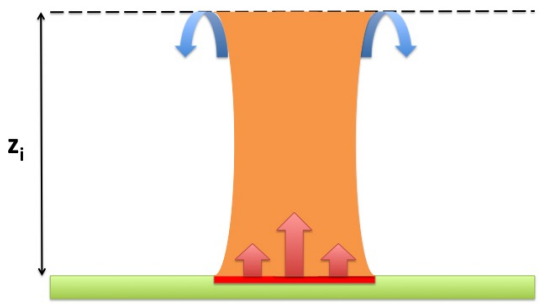

Figure 1: Thermal updraft and Convective boundary layer thickness z_i

2 Thermal Updraft Models

During daytime when the ground gets heated up due to the sun's radiation, the temperature of the ground rises. This results in heat transfer between the ground and the air close to it. This heat transfer is mainly conductive in nature. Due to differences in the nature of the ground, different regions get heated up differently resulting in areas called hot spots. Usually this will be a parking lot close to forest areas, farmland surrounded by trees etc. As the air in these areas have higher temperature than that of the surrounding air, convection current is set up causing this air to rise. The rising air exchanges heat with the surrounding atmosphere. This air rises over several hundred meters until it cools down and mixes with the surrounding atmosphere. The height until which this phenomenon happens is called the convective mixing-layer thickness z_i shown by the Figure 1.

The type of updraft shown in Figure 1 is also called as chimney thermal and is predominant in the absence of high horizontal winds. In the presence of high horizontal winds the rising air might get detached and start traveling along with the wind and this type of thermals are called Bubble thermals. More about them in section 2.9.

Various models can be found in the literature to describe this phenomenon and the main model features of a thermal are its radius and the updraft field. Both these variables as a function of altitude are studied. The updraft field representing how the vertical airspeed varies with the position relative to the thermal center, and its radius defining where the updraft speed is null or almost null, are the variables of main concern.

2.1 Overview

Lenschow [11] in 1980 performed experiment by taking humidity measurements over sea and formulated expressions for updraft velocity, diameter of the thermal and various other parameters as a function of vertical height. His analytical expressions are cited by all the other authors as well and hence serve as a basis for general updraft study. The model expresses statistical mean and variances of updraft velocity and diameter, for a given normalized thermal height based on measured data. His equations give variation of updraft velocity and thermal radius with altitude but assumes them to be constant in the horizontal direction. In this report his equations are extended to 3D by imposing a given profile on the updraft velocity showing the variation along the diameter of the thermal, hence in the horizontal direction.

M.J. Allen [1] puts forth a model based on balloon temperature readings and surface radiation measurements. The model is a mathematical representation of Chimney thermals in 3D. He develops his equations based on Lenschow's [11] work and based on flight test results from Konovalov [8]. This model gives the variation of updraft velocity with respect to height as well as with respect to the radius of the thermal. He considers the thermal as trapezoidal in shape. Using Lenschow [11] equation for the average updraft velocity and then

correlating this to the average velocity from the trapezoidal, he develops equations for updraft velocity at each point. The model also comprises of an environmental sink rate developed to conserve mass.

Childress [4] is based on collected data by flying at constant altitudes in and out of the thermals using an instrumented glider. A new phenomenon different from traditional plume rising thermals was observed using flight tests. The main difference between the conclusions of Childress and others is that, this author puts forth an idea of thermals with strong downdraft at the center of the thermal surrounded by maximum updraft regions. He says this kind of thermals with a core downdraft is formed when there are disturbances in the environment. The author maps the flight test data collected to a mathematical model forming equations based on Lenschow [11] and Allen [1].

Lawrance [10] Ph.D. thesis is about harvesting atmospheric energy for autonomous soaring using path planning. As the main idea is not on updraft modeling Lawrance in his Ph.D. thesis only briefly talks about a thermal model characterized by bubble formation. The author proposes detached thermal updrafts in the form of bubble leaving the ground in case of high winds. The model defines a 3D toroidal updraft flow field and the equations giving the wind velocity field at each location inside the bubble.

2.2 Lenschow's model

The study done by D.H. Lenschow and P.L. Stephans is one of the very first models proposed giving an analytical expression for the thermal updraft velocity and thermal diameter as a function of vertical distance. The equations proposed by Lenschow and Stephan, are used by all the other authors as a staring point in their own studies. Hence this paper forms as a basis for an updraft study. The equations in this paper are derived based on measurements taken using a NCAR Electra aircraft flying through convective boundary layer. All the results and conclusions of this paper are based on thermals formed over sea and not over land. The experiment consisted of flying the aircraft at constant altitude for 30km and measuring humidity changes. If the humidity change observed was more than half the standard deviation of humidity fluctuations, then the region was characterized as thermal.

The updraft properties derived are normalized to fit for any thermal irrespective of their height and surface heating, using scaling parameters w* the convective velocity scaling and, z_i convective mixing layer thickness. Based on the measurements, expressions are formed for the normalized number of thermals, diameter of the thermal and the updraft velocity.

The normalized number of thermals at regions close to the ground, $z < 0.2z_i$ was predicted to be a function of -1/3 powers of normalized height. For regions above this height the number of thermals are nearly constant.

For $z < 0.2z_i$,

$$N = 0.68(\frac{z}{z_i})^{\frac{1}{3}}$$

An expression is given for the diameter of the thermal as a function of 1/3 powers of normalized height,

$$d = z_i \times 0.16(\frac{z}{z_i})^{\frac{1}{3}}(1 - \frac{0.25z}{z_i}) \tag{1}$$

The average updraft velocity at any given height inside the thermal is given as a function of convective velocity scale parameter and normalized height by Equation 2.

$$\frac{\overline{w_T}}{w*} = 1.0(\frac{z}{z_i})^{\frac{1}{3}}(1 - \frac{1.1z}{z_i}) \tag{2}$$

In addiction to the above, an expression given by Equation 3 is also derived for temperature excess in the thermal.

$$\frac{\overline{\theta_T}}{\theta*} = 1.5(\frac{z}{z_i})^{\frac{1}{3}}(1 - \frac{2z}{z_i}) \tag{3}$$

From the mean updraft velocity and the temperature excess formed in the thermal, quantities such as the total contribution of heat flux of thermal, humidity excess, virtual temperature excess are also expressed in this paper. After expressing the mean quantities, the author extends his study by defining the variances of the calculated quantities as the function of normalized height also. The paper concludes by deriving an equation for mean vertical velocity equation for a thermal including the pressure and edge effect terms.

Hence this paper provides expressions for updraft and downdraft velocities, diameter of thermal, temperature excess and humidity excess in the thermal and the heat flux a function of normalized height. The variances of these quantities as a function of normalized height are also calculated. As this model comprises only on dependencies along the vertical direction it can be approximated as a 1D model for the thermals.

2.3 3D modeling of Lenschow equations

Lenschow model provides equations to calculate updraft velocity and thermal diameter at any given height but does not talk about the variation of those quantities along the horizontal direction.

The most basic modeling extension of thermals in 2D is Gaussian modeling of the vertical updraft velocity. This is done by imposing a Gaussian on the thermal with the maximum updraft velocity at the center of the Gaussian and the variance adjusted such that the vertical velocity at the end of the Gaussian is zero. This thermal profile has no downdraft associated to the thermal. This model can be seen in many previous work associated to autonomous soaring and modeling of thermals for such studies [15, 2, 5]. In this report and in the visualization model, this is done by assuming that the updraft velocity proposed by Lenschow as the core thermal center velocity and Lenschow diameter as the diameter of the Gaussian. Hence for a thermal with centerline updraft velocity w_core and radius R, the updraft velocity w at any given distance r from the center is given by Equation 4.

$$w = w_{core} e^{-(\frac{r}{R})^2} \tag{4}$$

Figure 2 shows the plot of Equation 4. The thermal was considered to axis-symmetric and this was extended to 3D in the visualization model and this can be seen in the Figure 3. As the Gaussian has no downdraft associated to it, Gedeon [7] proposed an improvement by adding a downdraft at the end of the Gaussian. In this model the thermal velocity is maximum at the center and becomes zero at the end of the thermal radius also but outside the thermal radius there is a region of downdraft where the vertical velocity is negative. This thermal profile is

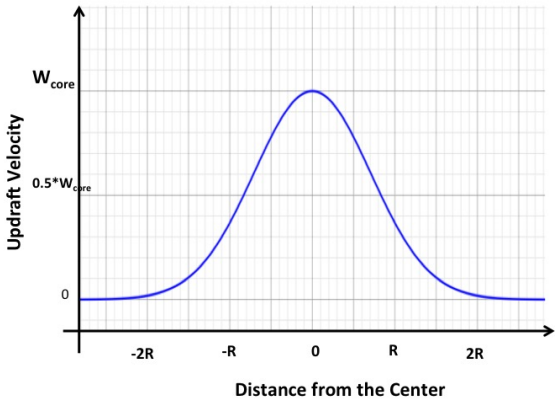

Figure 2: Variation of Updraft along the radius after imposing a Gaussian

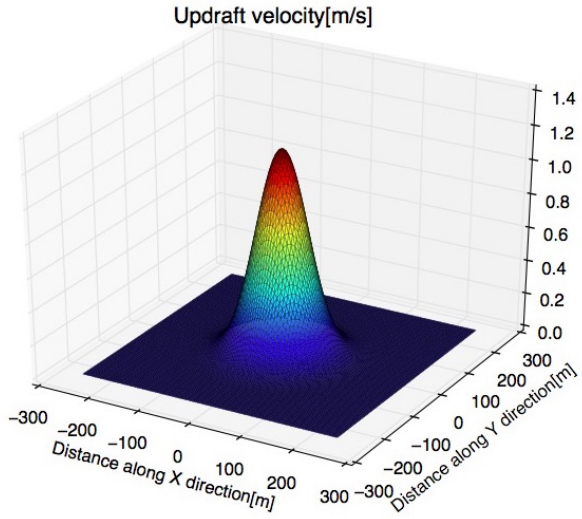

Figure 3: 3D representation of the updraft calculated by imposing a gaussian on Lenschow model

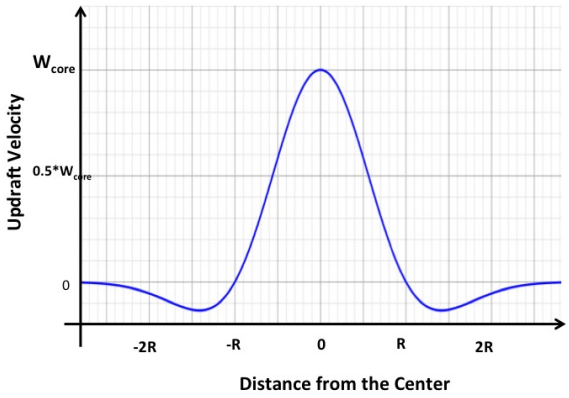

Figure 4: Variation of Updraft along the radius after imposing Gedeon's Profile

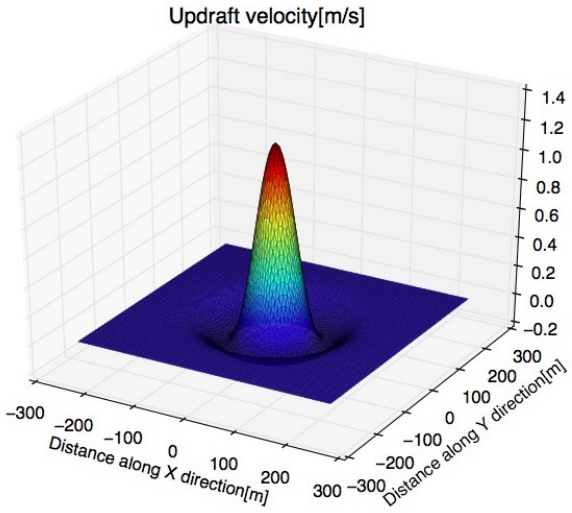

Figure 5: 3D representation of the updraft calculated by imposing Gedeon's profile on Lenschow model

widely used in many static soaring studies associated with [9, 12, 6]. Here the updraft velocity w at any given distance r from the center is given by Equation 5.

$$w = w_{core} e^{-(\frac{r}{R})^2} [1 - (\frac{r}{R})^2] \qquad (5)$$

The Figure 4 shows the 2D profile and Figure 5 the axis-symmetric 3D extension of the Gedeon equation.

The figures 6 and 7 show the variation of the Lenshcow models for different altitudes. It can be seen that as height increases the updraft velocity decreases but the effective radius of influence of the thermal increases. Though the effective radius of the thermal is the same between Gaussian distribution and Gedeon distribution, the decrease in updraft is steep in Gedeon model and also there is presence of downdraft at outer edge of the thermal. Hence for a location close to the thermal edge Gaussian imposed Lenschow model will produce a positive updraft while, for the same location Gedeon imposed Lenschow model will give a negative updraft.

Both the Gaussian and Gedeon approaches are pure empirical extensions of the lenschow models and the mass conservation of these approaches were not tested and validated. Also, the lenschow model does not give a smooth transition between the end of the convective layer z_i and heights above it. The

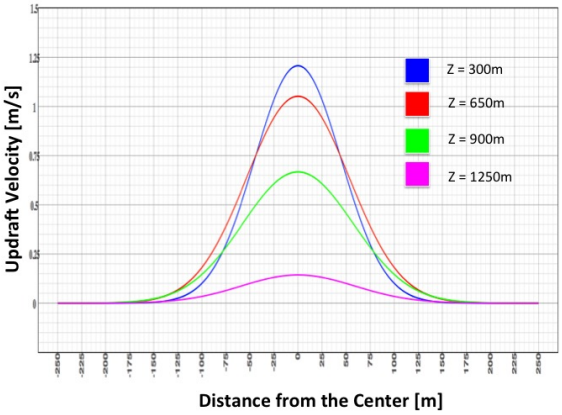

Figure 6: Variation of Updraft profile with Altitude for Lenschow with Gaussian imposed

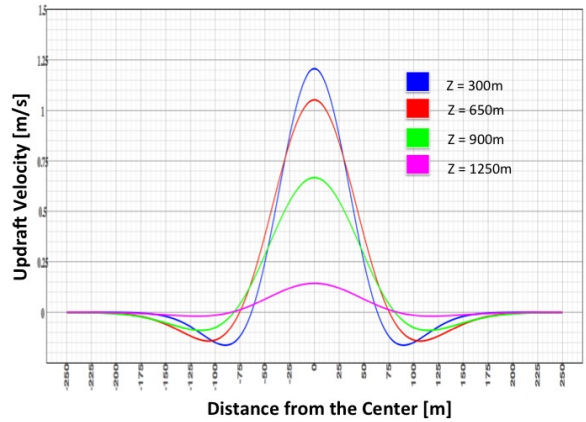

Figure 7: Variation of Updraft profile with Altitude for Lenschow with Gedeon imposed

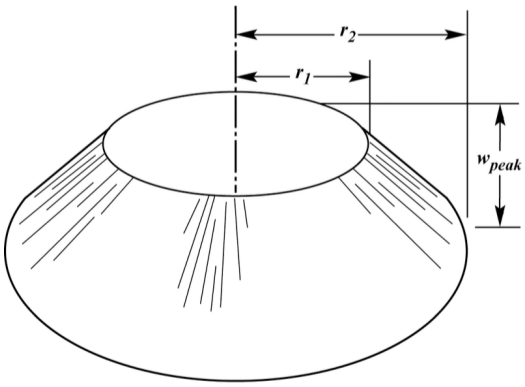

Figure 8: Updraft velocity distribution as revolved trapezoid from [1]

updraft velocity is maximum near the ground and it does not reaches zero when $z = z_i$. It reaches zero at approximately 0.9z* and then goes negative until the end of the convective layer. If the net updraft velocity outside the convective layer is considered as zero then this model, if used to perform soaring studies, will create a discontinuity when the altitude crosses the convective layer limit z_i.

2.4 Allen's model

M. J. Allen [1] collected data through surface radiation measurements and balloon-measured temperature over a year at Nevada, USA. The measurement consists of surface temperature, wind and radiation measurements using surface radiation station as well as temperature and humidity collected from balloon for an entire year of 2002. Using this data the primary observed and calculated quantities were, the convective velocity scale w* and the convective mixing layer thickness zi. The convective layer thickness zi is calculated by plotting measured balloon temperature and dry adiabatic lapse rate. Convective scale velocity w* is calculated using equations of sensible heat from Stull [14]. In this paper only conditions with horizontal winds less than 12.87 [m/s] (25 knots) are considered, for the rest w* is equated as zero. Equations from Lenschow [11] were used to calculate the average updraft velocity based on w* and zi. The equations used by Allen for the radius of the thermal has different coefficient compared to that of Lenschow [11].

Using the flight test results from Konovalov [8] this paper maps the relation between the radius of the thermal and updraft velocities. Thereby extending the model to 2D. Konovalov [8] shows that the maximum updraft velocity is not a single point but instead can be felt over a region in the center. This means that inside a thermal there will be a region with constant peak updraft velocity surrounded by a region of decreasing velocity until zero outside the thermal. To satisfy this Allen assumed the thermal to be having a revolved trapezoidal shape with peak updraft velocity at the center. The vertical velocity starts to decrease and reaches zero at the radius of the thermal. The revolved trapezoidal is shown below in Figure 8.

The updraft outer radius given by Allen is given by the Equation 6.

$$r_2 = \max(10, 0.102(\frac{z}{z_i})^{\frac{1}{3}}(1 - 0.25\frac{z}{z_i})) \times z_i \quad (6)$$

The average velocity given by Lenschow in Equation 2 is correlated with that of the area of the peak velocity and the volume of the entire trapezoid. Using that the peak velocity is given by the Equation 7

$$w_{peak} = 3\overline{w}\frac{r_2^3 - r_2^2 r_1}{r_2^3 - r_1^3} \quad (7)$$

As the height increases the thermal updraft velocity decreases and then turns into a downdraft.

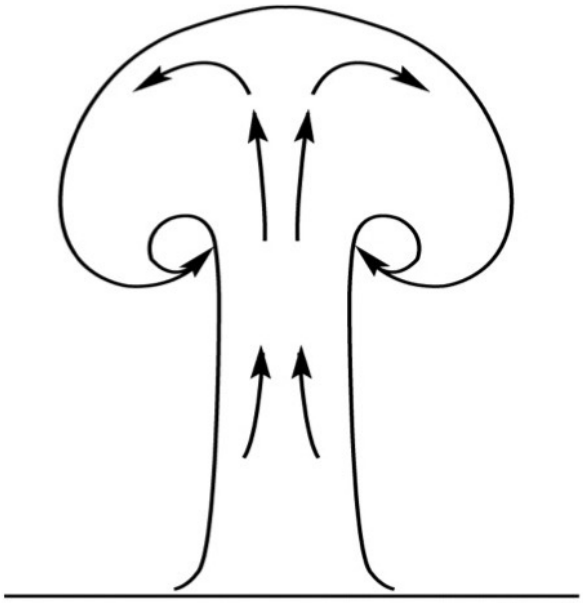

Figure 9: Toroidal Shape of the thermal from [1]

The toroid shape of the thermal showing this phenomenon is shown below in the Figure 9. Allen has developed equations for the downdraft developed as the height increases. The equations given by 8 and 9 are used to calculate the downdraft velocity.

$$w_l = \begin{cases} -\frac{\pi}{6}\sin(\pi \times \frac{r}{r_2}) & \text{for } r_1 < r < 2r_2 \\ 0 & \text{otherwise} \end{cases} \tag{8}$$

$$w_D = \begin{cases} 2.5w_l(\frac{z}{z_i} - 0.5) & \text{for } 0.5 < \frac{z}{z_i} < 0.9 \\ 0 & \text{otherwise} \end{cases} \tag{9}$$

To have a smooth transition between the peak updraft velocity in the thermal to the surrounding air, Allen has imposed a bell shaped curve based on shape constants k_{1-4} which depend on the radius ratio r1/r2 given by the table 1. The resulting profile for the updraft velocity for different bell shapes are shown in the Figure 10. To make the bell curves symmetric about r/r2=0 the constant k_3 was made zero in all cases. Based on all the above given characteristics the updraft velocity distribution along the radial direction is given by 10

$$w = w_{peak}(\frac{1}{1 + |k_1 \times \frac{r}{r_r} + k_3|^{k_3}} + k_4 \times \frac{r}{r_2} + w_D) \tag{10}$$

$\frac{r_1}{r_2}$	k_1	k_2	k_3	k_4
0.14	1.5352	2.5826	-0.0113	0.0008
0.25	1.5265	3.6054	-0.0276	0.0005
0.36	1.4866	4.8354	-0.0320	0.0001
0.47	1.2042	7.7904	0.0848	0.0001
0.58	0.8816	13.972	0.3404	0.0001
0.69	0.7067	23.994	0.5689	0.0002
0.80	0.6189	42.797	0.7157	0.0001

Table 1: Shape constants for different radii ratio

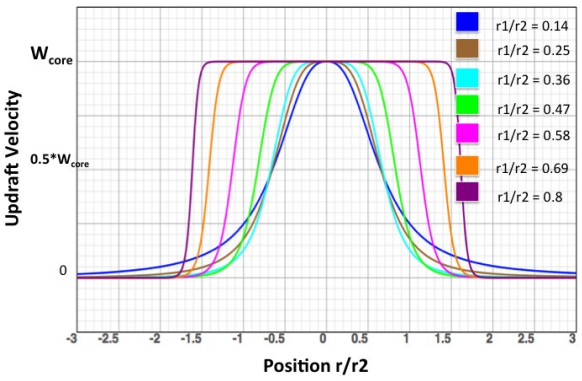

Figure 10: Bell curves for different shape constants

In a region of given area the maximum number of updrafts is computed using the equations from Lenschow [11]. For a given domain of horizontal area S, number of thermals N of height z_i and radius R is given by,

$$N = \frac{0.6S}{z_i R} \tag{11}$$

As updrafts are basically mass of air rising, to have conservation of mass equal about of mass has to descend. This paper also puts forth the environmental sink rate caused by a given number of thermals in a particular terrain. The resulting downdraft velocity in areas where there is no thermals is given by Equation 12.

$$\begin{aligned} w_e &= \frac{-\overline{w}\mathrm{N}\pi {r_2}^2 s_w d}{S - N\pi r_2^2} \\ s_w d &= \frac{w_D}{w_l} \end{aligned} \tag{12}$$

To have a smooth transition from the calculated updraft in the center to the environmental sink rate Equation 13 is used.

$$w_{total} = w(1 - \frac{w_e}{w_{peak}}) + w_e \tag{13}$$

2.5 Discussion on Allen's model

Figure 11 shows the updraft velocity for different altitudes. It can be seen that the updraft velocity decreases with altitude and the radius of the thermal increases with height. The negative velocity outside the Thermal is the environmental sink rate. Here while calculating the environmental sink rate, it was considered that one thermal is present in a region of 300x300 $[m^2]$ area. Figure 13 shows the 3D profile of the updraft velocity calculated using allen model at an altitude of 800[m]. The environmental flow rate calculated by Allen is done by applying mass conservation for every altitude i.e. if a slice is made at any given altitude then the amount of mass going upward in the form of the updraft is equal to the amount of air going down as down as downdraft. Because of this kind of modeling the environmental sink rate invariable becomes a function of altitude. Figure 12 shows the variation of environmental sink rate with respect to altitude.

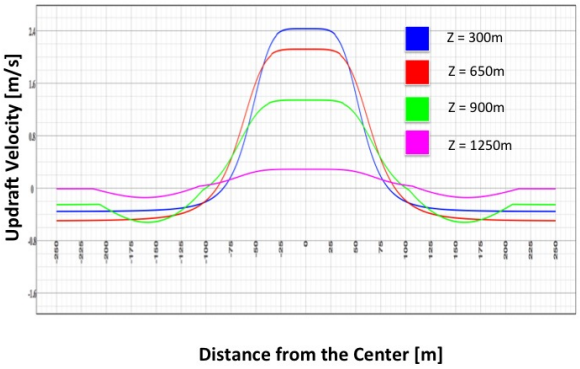

Figure 11: Allen updraft velocity profile for various altitudes

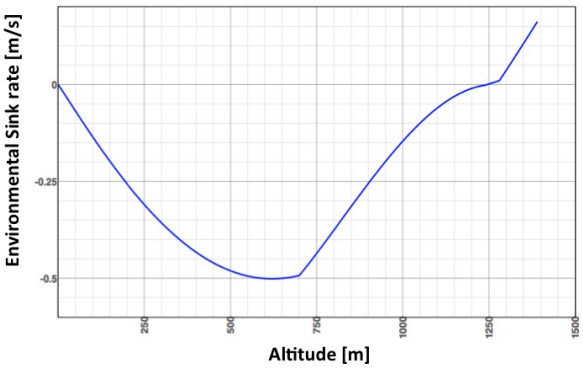

Figure 12: Variation of environmental sink rate with altitude

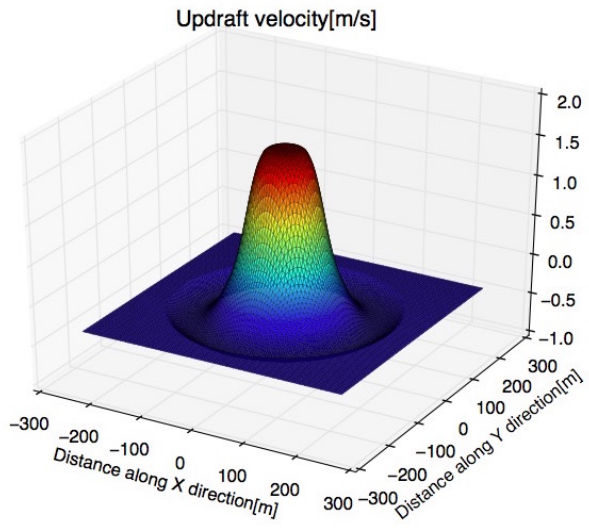

Figure 13: 3D representation of Allen updraft velocity at z=800[m]

2.6 Allen's model with ambient wind (Bencatel's model)

In the presence of horizontal winds the shape and position of the thermal updrafts may be disrupted. Thermal updrafts are formed over surfaces called hotspots. These hotspots depend on the topography of the terrain and because of which, the thermals remain anchored to this location. In most cases with horizontal winds, the thermal center on the ground does not drift along with the wind. This causes the thermal to drift along the direction of the blowing wind. In his report Allen says that his model is valid for horizontal winds less than 12.87[m/s] but he mentions no effect on winds below this value. To include the effect of winds into the Allen model equations from Bencatel [3] is used. Bencatel [3] states that, when the thermal is anchored to their hotspot or if the thermal drifting is slower than the wind speed, the thermals have tendency to lean along the wind. He has mentioned equations using which the leaning can be calculated.

In our model we have included the equations from Bencatel [3] to calculate the leaning of the thermal. The drift velocity of the thermal center near the ground can be modeled either as zero or a constant. The leaning of the thermal is characterized as thermal centerline leaning towards the wind. The centerline drifting is a function of the updraft velocity; if the updraft velocity is high the drifting is less. The following Equation 14 , 15 gives the position of the centerline at any given height based on wind velocity in the horizontal direction W_x and W_y.

$$x_t(H) = x_c + \int_0^H \frac{W_x(h) - u}{\overline{w_z}(h)} dh \qquad (14)$$

$$y_t(H) = y_c + \int_0^H \frac{W_y(h) - v}{\overline{w_z}(h)} dh \qquad (15)$$

Where, $x_t(H)$ and $y_t(H)$ are position of thermal centerline at height H, x_c and y_c are the position of thermal center on the ground, $W_x(h)$ and $W_y(h)$ are the ambient wind velocities in X and Y directions, $\overline{w_z}(h)$ is the average updraft velocity of the thermal as a function of height and u, v are the velocity with which the thermal center on the ground drifts. The drift velocities u, v in most cases assumed to be zero. Figure 14 shows the leaning of thermal center line along the direction of wind and Figure 15 shows the contour of the updraft with horizontal winds.

In case of thermals formed over sea or dessert with very even topography, this drift velocity can be assumed to be equal to the wind velocity, in which case the thermal only drifts and does not lean.

2.7 Childress' model

C.E. Childress, An Empirical Model of Thermal Updraft, [4] is characterized by taking measurements from an instrument glider flying in and out of thermals at different altitudes and comparing them to the traditional view of thermals as a single rising plume. From the data collected arguments were put forth saying that the thermal cannot be considered as a single rising plume after a certain height but instead another phenomenon, expressed as convective cells, is occurring. The paper builds mathematical models based on work by Allen [1] and Lenschow & Stephens [11].

The convective cell phenomenon expressed here refers to a cell that is formed when there is asym-

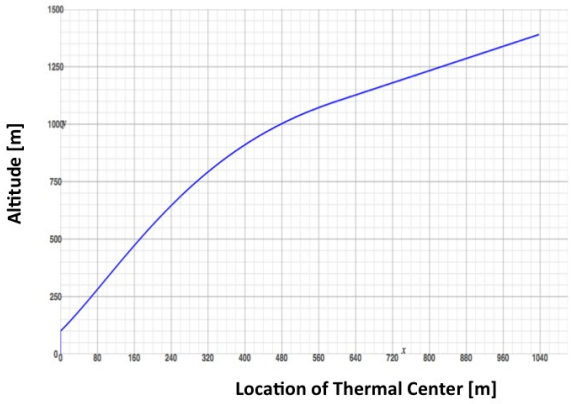

Figure 14: Leaning of Thermal Centerline with horizontal Wind

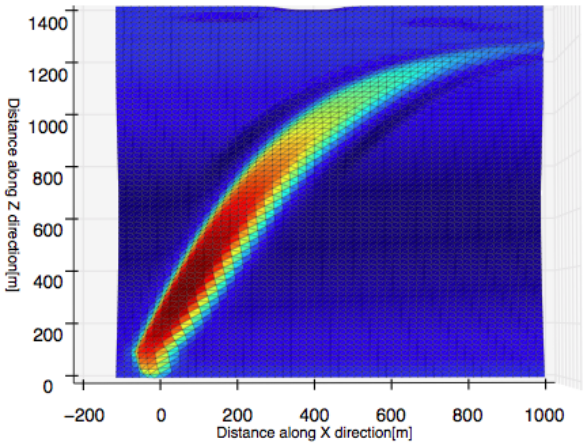

Figure 15: Updraft Contour in the presence of Horizontal Wind

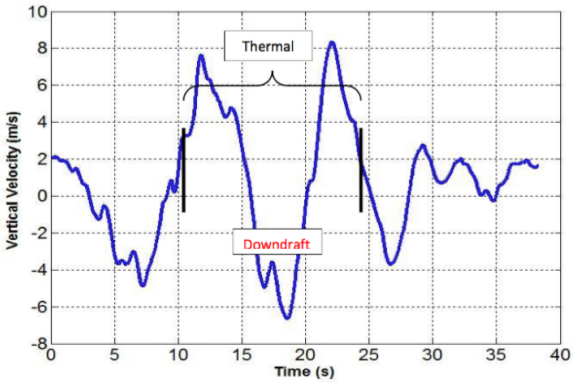

Figure 16: Measured Updraft velocity by Childress at z*=0.87 from [4]

metry or disturbances in the atmosphere. This phenomenon is prominent at heights above half the over all height of the Convective Boundary Layer (CBL). Above 50% CBL the thermal is no more single toroid shape with strong core section but instead two peaks with maximum updraft surrounding a core with strong downdraft. This core collapse phenomenon is a conclusion based on the data collected which is shown below. The quantity z*=current altitude(z)/height of CBL(z_i) Figure 16 shows one of the flight test data collected by Childress at z*=0.87 showing the updraft velocity. It can been seen here that a downdraft region is surrounded by regions of updraft.

With the data collected and based on equations from Lenschow the author develops equations for the diameter of the thermal and the diameter of the downdraft core as functions of vertical height. Based on measurement the author gives his validation on Lenschow model. It is shown that the diameter calculated using lenschow equations are three times smaller than the ones measured by the experiment. To account for the increased diameter the author used the same equations of lenschow but with different constants. The author also adds an additional term to account for the convective cell growth. The diameter of the thermal is given by the Equation 16.

$$d_T = z_i \times (0.4\sqrt[3]{z^*} \times (1 - 0.5z^*)) + \frac{(z^* - 0.6)(z^*)z}{\pi} \tag{16}$$

The paper also calculates the diameter of the core downdraft. The equation for the core downdraft diameter is given by 17.

$$d_1 = 0.17 d_T + 0.5 \times (z^* - 0.6) \times d_T \tag{17}$$

The updraft velocity along the vertical and radial directions is calculated based on the equations used by Allen [1]. Same methodology as that of Allen is adapted to find the peak velocity at the thermal center as a function of height. In addiction the downdraft velocity at the convection cell core is calculated using dimensionless decelerating term from Lenschow [11]. The core downdraft velocity as a function of dimensionless decelerating term w_d and the peak updraft velocity w_{peak} is given by 18.

$$w_D = w_d(z^* + 0.45) - 0.5 w_{peak} \tag{18}$$

The variation of vertical velocity along the radial direction is not derived based on experimental data but it is done by mathematically imposing an equation. The mathematical model imposed here can be hence divided into three, one for z* less than 0.5, another for z* between 0.5 and 0.9 and the third to characterize the region where the thermal dies out z* greater than 0.9.

For $z^* < 0.5$,

$$w(r) = w_{peak} \cos(\frac{r}{r_2} \times \frac{\pi}{2}) \tag{19}$$

For $0.5 < z^* < 0.9$,

$$w(r) = \begin{cases} w_D \times \cos(\frac{r}{r_1} \times \frac{\pi}{2}) & \text{for } 0 < r < r_1 \\ w_{peak} \times \sin(\frac{r - r_1}{r_2} \times 1.212\pi) & \text{for } r_1 < r < r_2 + r_1 \end{cases} \tag{20}$$

For $z* > 0.9$,

$$w(r) = \begin{cases} \frac{w_D}{2} \times \cos(\frac{r}{r_1} \times \frac{\pi}{2}) & \text{for } 0 < r < r_1 \\ (1 - z^*) w_{peak} \times \sin(\frac{r - r_1}{r_2} \times 1.212\pi) & \text{for } r_1 < r < r_2 + r_1 \end{cases} \tag{21}$$

A comparison of the Childress equation with the observed data can be found in Childress [4].

2.8 Discussion on Childress' model

Figure 17 shows the output of the Childress model for different altitudes. It can be seen that the effective area of the thermal increases with altitude i.e. the thermal radius increases with altitude. In the domain where the thermal is considered as traditional plume (region below $z^* < 0.5$) as height increases the updraft velocity decreases and the radius of the thermal increases. The variation in updraft velocity is significantly higher compared to Lenschow model. Also, the absolute peak updraft velocity in higher in Childress model than Allen and lenschow models. In the region where the convective cell phenomenon is observed. Both the updraft and the downdraft velocities decrease with altitude. The updraft smoothly reduces and become zero at z*=0.9 while the downdraft continue to decrease until $z^* = 1$. The radius of the downdraft core increases with respective to altitude. At which point there is still some downdraft. It should be noted that there is a strong discontinuity at the center line when z* is 0.5, 0.9 and 1. Figure 18 shows the variation of outer radius and the inner radius of the thermal with respect to altitude. Figure 26 shows the variation of centerline velocity with respect to altitude.

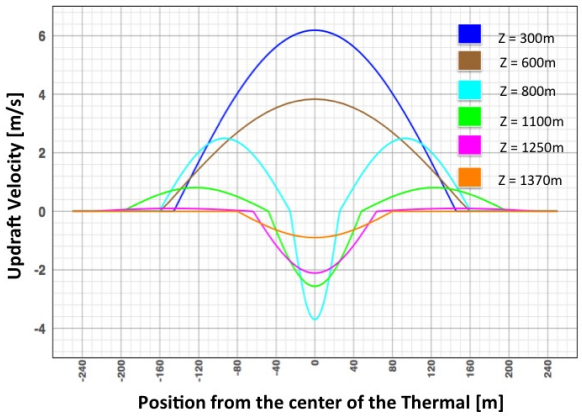

Figure 17: Childress vertical velocity profile for various altitudes

2.9 Lawrence's model

Lawrance [10] talks about thermals that are caused in places where there are high horizontal winds. This kind of thermal, due to the winds get detached from the ground and start rising independently in the form of a bubble, as shown in the Figure 20. They can be classified as bubble thermals and are

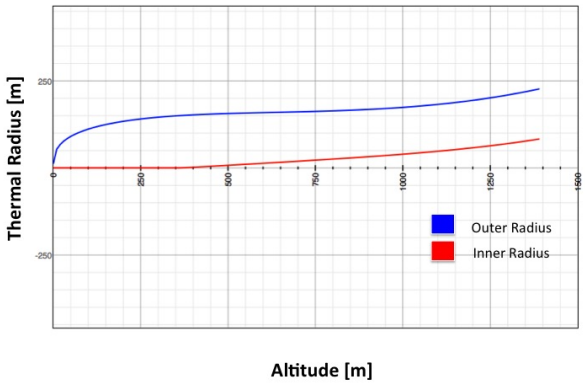

Figure 18: Variation of Childress thermal radius with altitude

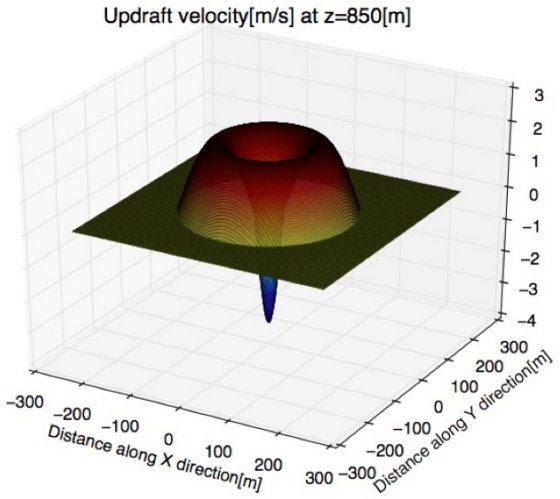

Figure 19: 3D representation of Childress updraft velocity at z=850[m]

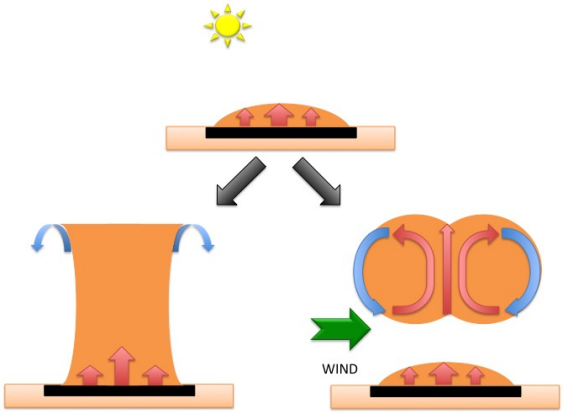

Figure 20: Formation of Bubble thermal

not continuous rising air mass like chimney thermals.

This kind of thermal is previously studied by Young [16] and the average updraft velocity as the function of height is given by 22.

$$\frac{\overline{w_T}}{w^*} = 0.85(\frac{z}{z_i})^{\frac{1}{3}}(1.3 - \frac{z}{z_i}) \tag{22}$$

The resulting updraft can be seen as a bubble detaching from the earth surface having a doughnut shaped with updraft at the middle and downdraft along the outer surface. The model defines a 3D toroidal updraft flow field given by the Equations 23, 24, 25. The Figure 21 from the reference [10] shows the thermal in space.

The velocity of wind along the directions X, Y, Z inside the thermal is a function of the distance from the thermal bubble center. If x, y, z are the distance from the bubble center then the velocity field is given by,

$$w_x = \begin{cases} \frac{w_z zx}{d_h(d_h - R)k^2} & \text{if } d_h \neq 0, R \\ \frac{w_{core}}{2k^2 R}(1 + \cos(\frac{\pi z}{kR})) & \text{if } d_h = R \\ 0 & \text{if } d_h = 0 \end{cases} \tag{23}$$

$$w_y = \begin{cases} \frac{w_z zy}{d_h(d_h - R)k^2} & \text{if } d_h \neq 0, R \\ \frac{w_{core}}{2k^2 R}(1 + \cos(\frac{\pi z}{kR})) & \text{if } d_h = R \\ 0 & \text{if } d_h = 0 \end{cases} \tag{24}$$

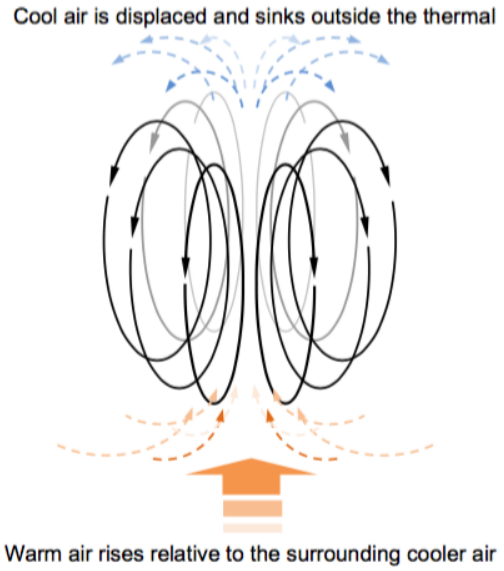

Figure 21: Shape of the Bubble thermal given by [10]

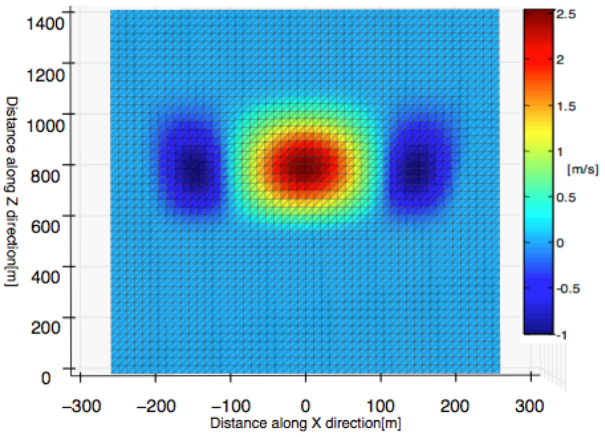

Figure 22: Updraft Contour of a thermal bubble centered at z=800[m]

$$w_z = \begin{cases} w_{core} & \text{if } d_h = 0 \\ \frac{w_{core} R}{\pi d_h} \sin(\frac{\pi d_h}{R}) \frac{1+\cos(\frac{\pi z}{kR})}{2} & d_h \in (0, 2R] \\ 0 & \text{if } |z| > kR \end{cases} \tag{25}$$

Where, w_{core} is the centerline updraft velocity, R is the radius of the thermal bubble, $k = \frac{\Delta z_{flow}}{2R}$ with Δz_{flow} is the vertical thickness of the bubble and d_h is the horizontal distance from the centerline given by $d_h = \sqrt{x^2 + y^2}$.

Figure 23 shows the wind vector for every point inside the thermal bubble developed using Equations 23, 24 and 25. For a thermal bubble positioned at z=800[m] Figure 22 gives the updraft velocity distribution. The toroidal shape of the bubble thermal can be clearly observed. The radius of the thermal and the peak velocity are calculated based on Section 2.4.

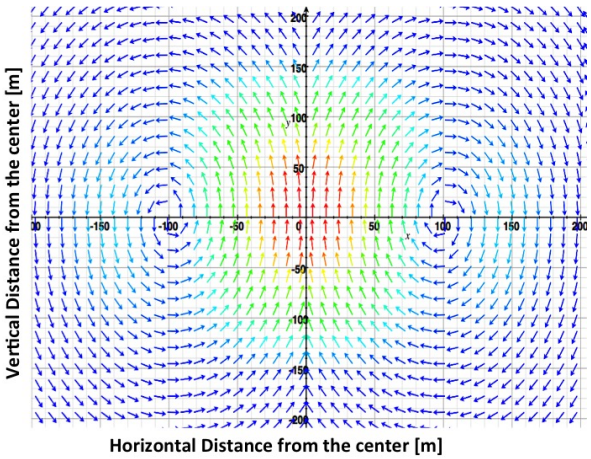

Figure 23: Wind vector inside a Bubble thermal

3 Comparison of models

Figure 24 shows the comparison of updraft velocity profile of all the thermal models at an altitude of 600[m] for the same w* and z_i. It can be seen that though the convective velocity scale w* is the

same, the updraft predicted by the models are very different. The Updraft given by Childress model is higher than all the other models, while that predicted by Lenschow is the least. It can be argued that as Lenschow [11] is based on measurements from updrafts formed over the sea, the predicted updraft velocity is lower than the rest. Due to the environmental sink rate allen model gives a constant downdraft everywhere outside the thermal. The downdraft given by Gedeon [7] can be compared to the immediate downdraft around the thermal, formed due to the air being sucked near the ground by the growing thermal. Lawrance bubble thermal with center position at 600[m] is modeled using equations from Allen hence the peak updraft velocity and the radius of the thermal are same as that of Allen. But it can be clearly seen that the toroidal bubble of Lawrance prroduces more downdraft compared to others. This is because the bubble is characterized by more circulating air. When seeing the updraft profile at z=900[m] show by the Figure 25 the differences in magnitude of the updraft between the different models still holds i.e. Childress is higher than all the other models and lenschow updraft remains the lowest. But the shape of the updraft is different between Childress and Allen. The convective cell formation is prominent in Childress model while the excess downdraft formed outside the thermal in Allen is due to the shape of thermal shown in Figure 9. Figure 26 shows the variation of centerline velocity with respect to height for the different thermal models and Figure 27 the variation of thermal outer radius with respect to height. The Lawrance bubble thermal is modeled to move up with w_{core} and radius R as that of Allen. Hence, in both these cases the Lawarance bubble thermal, produced the same results as that of Allen.

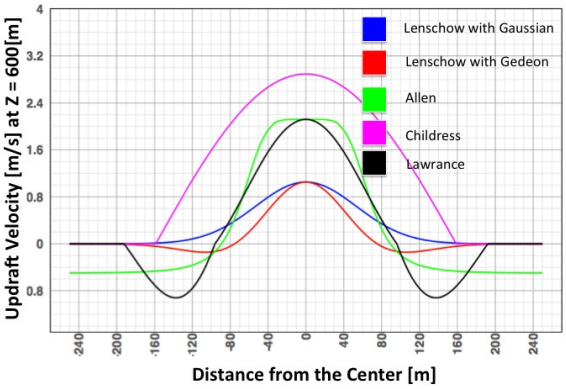

Figure 24: Comparison of Models at z=600[m]

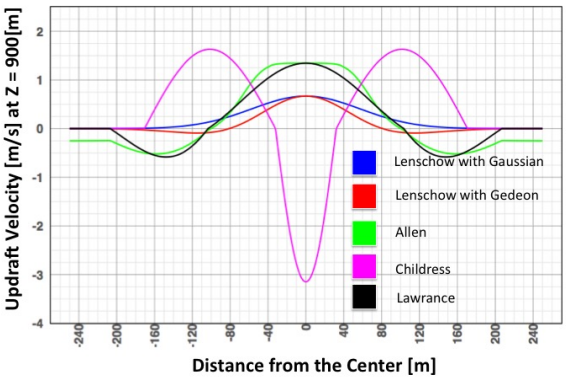

Figure 25: Comparison of Models at z=900[m]

4 Thermal Life Cycle

When thermals are formed, each thermal undergoes a specific lifecycle. A thermal lifecycle consists of creation, a resting or formation phase, a growing phase, a matured phase, a fade off phase and death. The time taken to heat the air around the regions of hotspot until a natural convection current is formed can be termed as resting phase. During this phase the location of the thermal is known

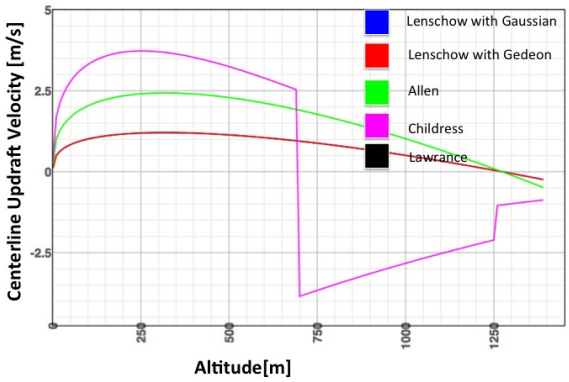

Figure 26: Comparison of Center line updraft velocity

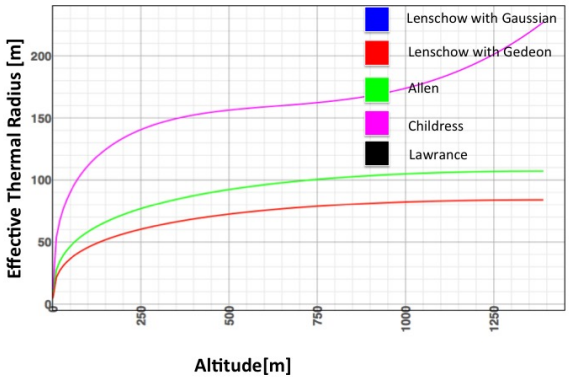

Figure 27: Comparison of Thermal Radius

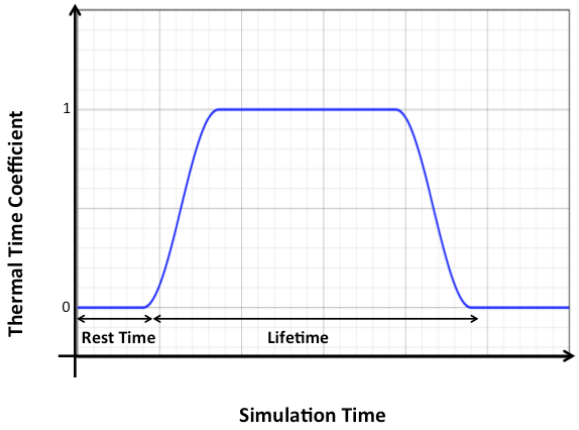

Figure 28: Evolution of time coefficient

but as the thermal is not yet developed it has no updraft. Once the thermal starts rising upward, the time taken to achieve its maximum updraft velocity can be termed as the growing phase. Once the thermal is matured it continues to have maximum updraft velocity. This is usually during the date time or when then sun is at the peak. Once the environment cools down the thermal slowly fades out and dies. To model the thermal life cycle a multiplication factor or the time coefficient given by the following graph show in the Figure 28 is used. This thermal time coefficient varies from zero to one, zero representing no effect of the thermal and one representing the maximum effect of the thermal. The thermal time coefficient is multiplied to the updraft velocity to get the effect of Thermal life cycle. If t_{Sim} is the simulation time and t_{rest} and t_{life} are the resting and lifetime of the thermal then the thermal time coefficient is calculated using Equation 26 from [13].

$$c = \begin{cases} 1 & \text{if } \|\tau\| \leq D, \\ \frac{1}{2}[1 + \cos(\frac{\pi T}{\xi}(|\tau| - D))] & \text{if } D < |\tau| \leq \frac{1+\xi}{2T}, \\ 0 & \text{else} \end{cases} \tag{26}$$

Where,

$$\tau = t_{sim} - (t_{rest} + \frac{t_{life}}{2}) \tag{27}$$

$$D = \frac{1 - \xi}{2T} \tag{28}$$

$$T = \frac{1+\xi}{t_{life}} \tag{29}$$

The factor ξ is the parameter that defines the shape of the function, randomly chosen for each thermal.

5 Windfield Generator

The computerized tool created along with this report is developed using C++ language. It is parametric in nature, meaning that it operates on a given set of parameters and on analytical equations. This tool can be used to include the effects of randomly formed thermals on a given domain. The input variables for the program are position and time. The output will be wind vector at the given point and time.

Inside the program a wind field is generated. A wind field is a given domain in space with dimensions specified. Inside the wind field, thermals will randomly form and vanish. A scenario file is created or loaded from an existing file at the beginning of the simulation, which consists of dimensions of the domain, the minimum and maximum simulation time and the ambient wind in the horizontal axis in the absence of thermal. Each thermal information consists of the location at which the thermal will be formed, the convective velocity scaling parameter w^*, time at which the thermal will be formed and the lifetime of the thermal. The effect of the thermals on the aircraft is based on the model chosen. The output wind vector will be the superposition of the ambient wind and the effect of thermals. The effect of thermal once calculated based on the chosen model is multiplied by the thermal time coefficient to take into account the lifecycle of the thermal. The number of thermals at any given instant of time is decided based on the equations given by Lenschow [11] and Allen [1] as given by Equation 11.

To show the working of the software tool the scenario file shown in Figure 29 in the form of a `.txt` file is loaded to the program. Any line with # is read as a comment. But the order of the given data should be respected as the program reads the data line by line. After the general domain characteristics, the information regarding the thermal is added continuously. This consists of the center position of the thermal and the time characteristics. This is read till the end of the file. The program

```
# Definition of the domain :
# MinX and MaxX
0 2000
# MinY and MaxY
0 2000
# MinZ and MaxZ
0 1400
# Starting and Ending time of simulation
0 100
# MinLifeTime and MaxLifeTime of Thermal
10 14
# MinRestTime and MaxRestTime of Thermal
0.2 2
# Ambient WindX and Ambient WindY
0 0
# Convective Mixing layer thickness
1400
# The list of Thermals created :
# CentreX   CentreY   wStar   tBirth   tRest   tLife
937.975 1049.15 3.64 0 1.56009 10.5262
1268.94 1652.04 3.64 0 1.42196 10.1882
301.858 330.192 3.64 0 1.69574 12.0777
825.123 350.263 3.64 0 0.213857 12.6846
1393.3 643.679 3.64 0 1.26016 12.7471
620.558 1723.83 3.64 0 0.790822 12.9443
359.029 1197.45 3.64 12 1.37273 13.0134
788.897 499.761 3.64 13 0.985541 11.0908
```

Figure 29: Configuration file containing all the information about the Windfield

reads this file and creates a wind field object. The wind field object can also be created without loading the scenario file but just the domain parameters. Using the domain parameters the thermals will be created automatically and randomly over the domain by the program, respecting the Equation 11 at any given time. Using functions defined within this wind field object, one can obtain the wind vector for a given point at given time.

An example code to include the software tool and showing the usage is shown below. The header file "WindField.hpp" contains the class "Windfield", whose members and methods are used to create the wind field with thermals, and which can be used to get the wind vector using the function `calcwind(x,y,z,t)`. To create a windfield object the user can either use default parameters or parameters from a file. In the code below the object `windfld` is created automatically using the default parameters for the domain and the object `windfld2` is created from the file `"config.txt"`.

```
Windfield windfld;
Windfield windfld2("config.txt");

double wind[3];
double t=8.0, x=300.0,y=300.0,z=650.0;
```

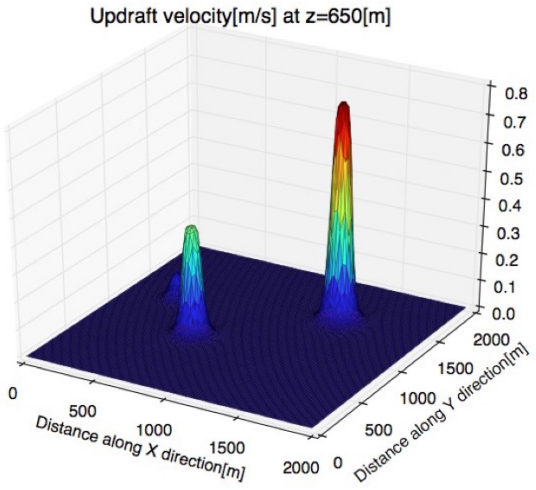

Figure 30: Windfield showing updraft at Z=650m at time "t" seconds

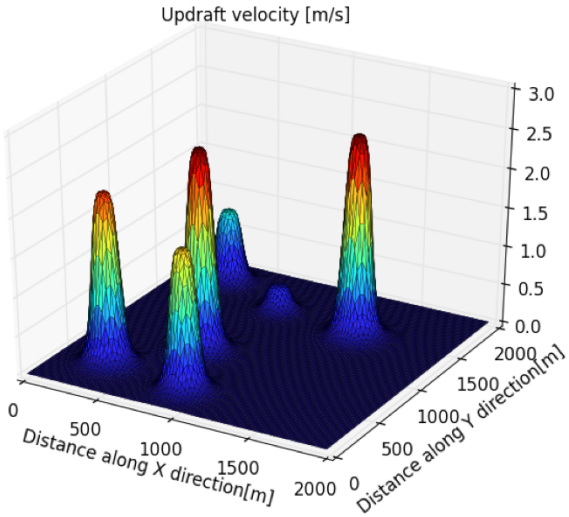

Figure 31: Windfield showing updraft at Z=650m at time t+2 seconds

```
wind=windfld.calcwind(t,x,y,z);
```

Using the calcwind function the value of wind can be calculated at any point and time. It was done for the entire domain and the Figure 30, 31, 32 below show the vertical velocity at every point in the windfield. The updraft velocity was calculated using Allen [1] model. All the thermals have the same characteristics and hence will result in the same updraft velocity, for a given height. Here it is calculated at the height of 650m. However, at a given time all thermals have same updraft velocity this is because of the thermal time coefficient. It can be seen that some thermals are fully developed and some of them are still in the developing phase characterized by lower vertical velocity. The three pictures shown here are the wind field statuses at time `t, t+2, t+4` seconds.

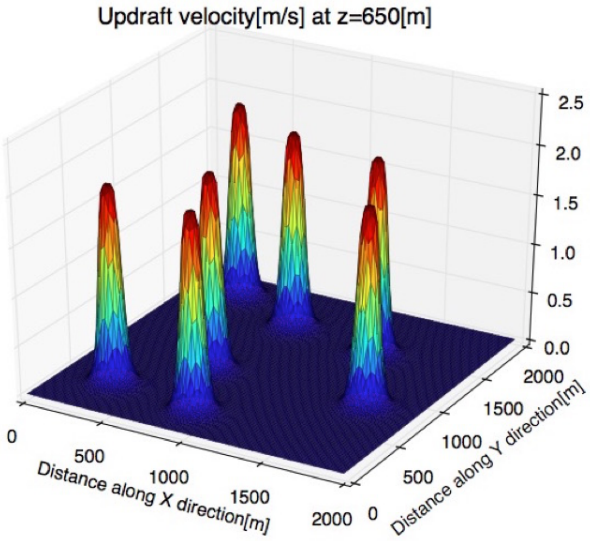

Figure 32: Windfield showing updraft at Z=650m at time t+4 seconds

6 Conclusion

This survey puts forth the developments and research undergone in the area of thermal updraft modeling. The data collected and the equations used by Lenschow [11] can be applied to find the given number of thermals in any region along with the detailed variation of updraft velocity and di-

ameter for thermals with altitude. The imposed Gaussian and Gedeon [7] approach help in giving a 3D shape for vertical updraft velocity. Allen [1] has given a detailed 3D model of the thermals, which form the basis of Plume type revolved trapezoidal updrafts also called as Chimney Thermals. With the environment sink rate, [1] can be directly used to replicate thermal soaring studies without horizontal winds. The equations given by Bencatel [3] extend Allen [1] with horizontal winds and hence can be used to replicate thermal leaning and drifting. In regions where there is frequent merging of thermals, Childress [4] can be used to represent downdrafts surrounded by updrafts. The formation of convective cells over certain altitudes and data collected showing the same by [4], is a new phenomenon different from the traditional plume type thermal and hence can serve as a starting point for new research. The thermal bubble phenomenon proposed by Lawrance [10] is a good approximation to model thermals formed over regions with high winds and that are highly disrupted.

As it is clearly visible the sophistication and complexity in modeling thermals has increased chronologically. The naturally occurring updrafts are extremely complex and depend on several other natural, turbulent and unknown atmospheric phenomena. Hence it is impossible to create a mathematical model taking into account all of them. However, the above references can provide a very good approximation and can be used directly. Future work can be done to come up with new theories and, theories based on the mentioned work to capture the real world occurrences as close as possible.

References

[1] M. J. Allen. Updraft model for development of autonomous soaring uninhabited air vehicles. Technical report, NASA Dryden Flight Research Center, 2006.

[2] K. Andersson and I. Kaminer. Stability of a thermal centering controller. In *AIAA Guidance, Navigation, and Control Conference,(Chicago, Illinois), AIAA*, 2009.

[3] R. Bencatel, J. T. de Sousa, and A. Girard. Atmospheric flow field models applicable for aircraft endurance extension. *Progress in Aerospace Sciences*, 61:1–25, 2013.

[4] C. E. Childress. An empirical model of thermal updrafts using data obtained from a manned glider. Master's thesis, University of Tennessee - Knoxville, 2010.

[5] D. J. Edwards. Implementation details and flight test results of an autonomous soaring controller. In *AIAA Guidance, Navigation and Control Conference and Exhibit*, pages 18–21, 2008.

[6] C. Gao. *Autonomous soaring and surveillance in wind fields with an unmanned aerial vehicle.* PhD thesis, University of Toronto, 2015.

[7] J. Gedeon. Dynamic analysis of dolphin style thermal cross-country flight. In *Proceedings of the XIV OSTIV Congress, Organisation Scientifique et Technique Internationale du Vol à Voile*, 1974.

[8] D. A. Konovalov. On the structure of thermals. Technical report, Main geophysical Observatory, Leningrad, USSR, 1970.

[9] J. W. Langelaan. Gust energy extraction for mini and micro uninhabited aerial vehicles. *Journal of guidance, control, and dynamics*, 32(2):464–473, 2009.

[10] N. R. J. Lawrance. *Autonomous Soaring Flight for Unmanned Aerial Vehicle.* PhD thesis, University of Sydney, 2011.

[11] D. H. Lenschow and P. L. Stephens. The role of thermals in the convective boundary layer. *Boundary-Layer Meteorology*, 19(4):509–532, 1980.

[12] Y. Qi and Y. J. Zhao. Energy-efficient trajectories of unmanned aerial vehicles flying through thermals. *Journal of Aerospace Engineering*, 18(2):84–92, 2005.

[13] E. Rachelson, M. Melo, and S. Rapp. Development of a q-learning algorithm for improved autonomous soaring. Technical report, Institut Supérieur de l'Aéronautique et de l'Espace, Toulouse, 2014.

[14] R. B. Stull. *An Introduction to Boundary Layer Meteorology.* Kluwer Academic Publishers, 1994.

[15] J. M. Wharington. *Autonomous Control of Soaring Aircraft by Reinforcement Learning.* PhD thesis, Royal Melbourne Institute of Technology, 1998.

[16] G. S. Young. Turbulence structure of the convective boundary layer. part ii: Phoenix 78 aircraft observations of thermals and their environment. In *Journal of the Atmospheric Sciences*, 1988.